Available online at www.sciencedirect.com

jmr&t
Journal of Materials Research and Technology

journal homepage: www.elsevier.com/locate/jmrt

Original Article

Microstructural and thermal characterization of concretes prepared with the addition of raw and milled fly ashes

Jadambaa Temuujin [a,*], *Claus H. Ruescher* [b]

[a] *Mongolian Academy of Sciences, Peace Avenue 54b, Ulaanbaatar 13330, Mongolia*
[b] *Institute of Mineralogy, Leibniz University of Hannover, Germany*

ARTICLE INFO

ABSTRACT

The influences of mechanically activated fly ash on the microstructure and thermal behaviour of atmospheric-cured concrete panels have been evaluated. For this purpose, comparative analyses of concretes prepared with and without addition of raw and milled fly ashes were performed. The raw fly ash was activated with an attrition mill for 1 h. Cylindrical concrete specimens with and without 20% fly ash substitution and large concrete panels with the same compositions were prepared. Mechanical properties of the concrete specimens were measured after 3, 7, 28 days, 2 and 4 months. After preparation the cylindrical specimens were cured in water while the concrete panels were kept in an open atmosphere outside the building for 1 year.

The 28-day compressive strengths of the non-fly ash added cylindrical concrete specimen was 61.1 MPa, raw and mechanically activated fly ash added specimens were 54.4 and 64.7 MPa, respectively. Microstructural and thermal studies of the concrete panel were performed in the core drilled specimens after 1 year curing. The compressive strength of the core drilled specimens was 26.6, 25.4 and 35.9 MPa for the non-fly ash added, raw and mechanically activated fly ash added concrete panels.

A beneficial pozzolanic reaction and improved mechanical properties of the milled fly ash-substituted concrete cured under harsh weather conditions were observed and determined by differential thermal analysis-thermogravimetry and mercury intrusion porosimetry. Improved mechanical properties of the milled fly ash added panel indicates its potential applicability in industrial practice due to the simplicity of the process.

1. Introduction

Concrete is one of the most commonly used materials in human history. Concrete can be considered a hardened binder-phase mixture with fine and coarse-grained aggregates. The binder phase is generally composed of ordinary Portland cement (OPC) hardened by hydration. Although the history of the OPC started in the 1820s [1], the real OPC that

used rotary kiln with the controlled quality began after the 1900s. After that, the OPC is the main binder constituent in the concrete industry, with a production rate of 10 million tonnes in 1900 to 1500 million tonnes in 2000 [2]. Many different additives, including fly ash, have been shown to improve cement or concrete properties. Use of fly ash started in the 1930s, and very substantial research has been performed since then [3]. Fly ash can be used as an additive in OPC or concrete production. When fly ash is used for the OPC clinker as an additive, it is called CEM II type or Portland-fly ash cement [4]. Use of fly ash in the concrete shows positive influences such as low heat of hydration, high durability, high strength, and improved workability related to the extent of replacement [5,6]. With the addition of fly ash, the water content could be reduced, which results in a high packaging density and high strength [7].

The fly ash was used as a pozzolanic additive, and the calcium content of the fly ash also showed influences on the concrete composition and processing [8,9]. In fact, there are many thousands of research papers, including review papers, in recent years [10–13].

The property of fly ash as a pozzolanic additive depends on its chemical and mineralogical composition. The pozzolanic reaction is usually described as a secondary formation of the calcium-silicate hydrate (C–S–H) phase according to the reaction:

$$Ca(OH)_2 + Si(OH)_4 \rightarrow CaH_2SiO_4 \cdot 2H_2O \text{ (C–S–H)} \tag{1}$$
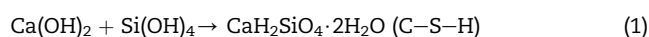
Certainly, in this reaction, fineness and breakdown of the glass structure of fly ash are essential factors to consider. Fineness and increased amorphization of the fly ashes can be reached by mechanical activation. Previous research by Kumar et al. [14,15] and by Temuujin et al. [7] indicates amorphization and improved reactivity of the fly ash with mechanical activation resulting in a better geopolymerization reaction by alkali activation. Bicer [16] and Han et al. [17] have noted that fly ashes with a fine particle size easily interacts with the alkaline liquid during the geopolymeric reaction, but also with the cement hydration products by pozzolanic reaction to form high strength cement and concrete products.

Kumar et al. [15] observed that mechanical activation of fly ash results in a significant increase in the early strength of cement as compared to commercial cement from one of the benchmarked cement plants. It was found that 50–60% mechanically activated fly ash can be used as a replacement for clinker with strength higher than, or comparable to, commercial cement. Based on hydration energy measurements, it was suggested that hydration of C_3S and C_3A is a crucial factor for increased strength development, though they used mechanically activated fly ash but not activated cement clinker. Strength development could be correlated with the microstructure of concrete and the content of the cementitious C–S–H phase. At the same time, C–S–H phase formation will depend on the rate of the pozzolanic reaction between the cement phase and fly ash. Since the pozzolanic reaction occurs slowly, the strength development in the ambient temperature cured specimens could show a relation between microstructure and cementitious phase in the fly ash added or raw concrete samples.

An improved reactivity with alkaline solution was reported for attrition and vibration milled fly ashes [18]. It was suggested that the attrition mill is a more suitable device for fly ash activation than the vibrating mill. With time, the compressive strength change resembles those obtained with OPC, ground and raw fly ash added mortar [19]. This was explained by a beneficial pozzolanic reaction in the ground fly ash added mortar. Blanco et al. [20] studied the influence of wet-milled and chemically leached fly ashes on the microstructure of cement mortars. They noted the mortar prepared with the addition of 10 and 20% of mechanically and chemically activated fly ashes had a higher strength after 7 days of curing and longer.

The reduction of the fly ash particle sizes can be achieved by either mechanical grinding or sieving. The former requires energy input but can be used on all of the fly ash and may induce mechanical activation, the latter only uses the finer fly ash resulting in a coarse residue.

It is important to note that the previous research used a standard curing procedure for the mortar preparation, i.e., initial curing in the curing chamber followed by submerging in water [19,20]. Such a traditional curing method allows production of specimens without any influence of dehydration or surrounding temperature fluctuations. In commercial practice, concrete panels are usually prepared on a construction site under uncontrolled ambient conditions. At this time, there are insufficient reports on the microstructure and related thermal reactions of fly ash concrete cured under atmospheric conditions with high temperature fluctuation over time. Therefore, the microstructural study of concretes prepared with and without the addition of mechanically activated fly ash and cured under ambient conditions allows the gathering of information necessary for strength prediction of the building and road concrete panels.

The aim of the present research is to evaluate the relationship between microstructure and the thermal reaction of the concrete cured under comparatively extreme atmospheric conditions for 1 year. It extends knowledge of the pozzolanic reaction mechanism between the milled or non-milled fly ashes and OPC under atmospheric conditions. Further, the methodology may be used for choosing an optimal milling condition.

2.   Experimental procedures

Fly ash from the 4th Thermal Power Station of Ulaanbaatar was used. Fly ash was used as received and after activation with an attrition mill. From previous research the energy efficiency of attrition mill expressed by grinding energy was much higher than the vibration mill. Therefore, for the present research was used fly ash milled by the attrition mill. The activation of the fly ash is described elsewhere [18]. With attrition milling the average particle size was reduced from 29 to ≈6 μm and density was increased from 2.44 to 2.84 g/cm³. The attrition mill shows particle size reduction effect without

Table 1 — Mix proportions of the concrete.

	Concrete, without fly ash addition	Concrete with 20% fly ash substituted	Concrete with 20% activated fly ash substituted
Cement (MAK350)[a], kg	567	453.5	453.5
Coarse aggregate, kg	1082	1082	1082
Natural sand, kg	1125	1125	1125
Fine sand, kg	615	615	615
Water, kg	247	229.1	229.1
Superplastisizer, kg	5.67	5.67	5.67
Fly ash, kg	−	113.4	113.4

[a] MAK350 means OPC produced by MAK LLC. for production of concrete with approx. 32 MPa compressive strength.

heavily distortion of the microstructure, i.e. minimal mechanical activation. The main difference due to attrition milling is a reduction in the particle size resulting in the high surface area.

2.1. Preparation of concrete

Concrete panels and specimens were prepared using the facility at the Premium Concrete LLC. in Ulaanbaatar. A total of 4.5 m^3 of concrete mixture were prepared using industrial equipment. From this mixture, concrete panels of 2400 × 1800 × 30 cm and cylinder specimens of 20 × 10 cm (height x diameter) were prepared. The mixing proportions of the prepared concrete samples are shown in Table 1 and follow the standard formula used in the concrete industry. Specimens and concrete panels were covered by a plastic sheet left in place for 1 day. After 1 day the cylindrical specimens were demoulded and kept in a water bath at 22 °C until testing (3, 7, 28 days, 2 and 4 months). The concrete panels were left in the air for 1 year. After 1 year specimens were taken by core drilling.

Slurry properties of the prepared concrete mixtures are shown in Table 2.

In the fresh slurry the fly ash addition results in a reduction in the air content and cone slump which are indicators of a denser microstructure. After 1 year of ambient temperature curing, neither damage nor cracks were observed on the panels.

2.2. Characterization

Chemical composition of the collected fly ash was measured by X-ray fluorescence (XRF) using the tetraborate fusion method. X-ray diffraction (XRD) pattern was measured by using Bruker D4 diffractometer with CuKα radiation between 5° and 80° 2Θ. Amorphous content of the concretes was determined semi quantitively by subtracting of the integrated area of crystalline compounds from the integrated area of the XRD of the sample.

The compressive strength of the cylindrical concrete samples was measured in a compressive testing machine Humboldt HCM-40000, Humboldt Mfg. Co. Specimens were tested in triplicate for compressive strength after 3, 7, 28 days, 2 and 4 months, respectively, the average value was applied as compressive strength value. The cylinder-shaped core drilled specimens were cut to have flat surface and had size of 20 × 10 cm. For compressive strength data were used average value of 2 specimens. The number of the specimens tested were not sufficient to make a statistically significant conclusion on the concrete panel's strength. There are many variabilities to show influences on the compressive strength. However, the 2 measurements were less than 20% apart, which is assumed to be significant as average value. Therefore, the strength of the concrete should be considered as the trend rather than true value.

Thermogravimetric (TG) and differential thermal analysis (DTA) measurements were carried out on the core drilled specimens left after the compressive testing. The measurements were performed using alumina crucible between 25 and 1000 °C with Seteram Setsys Evolution 1650, technical air with flow 20 ml/min and at 10 °C/min heating−cooling rate. After cooling the powders were analysed by IR.

The IR absorption spectra were analysed by Fourier transform infrared (FTIR) spectroscopy. The FTIR absorption spectra were measured in a Bruker, Vertex 80v spectrometer by KBr suspended disc method with 0.6 mg sample per 200 mg KBr. Spectra are shown in absorbance units (-lg (I/I$_0$)).

Table 2 — Prepared concrete slurry properties.

No	Properties	Values		
		Without fly ash addition	20% raw fly ash substituted	20% activated fly ash substituted
1	Cement	MAK M350	MAK M350	MAK M350
2	Cone Slump, MM	240	230	220
3	Air Content, %	4.2	3.0	2.5
3	Surrounding temperature, ^{0}C	28	28	28
4	Concrete temperature, ^{0}C	23.6	24	23.2

Table 3 – Chemical composition of fly ash and OPC, M350 (wt.%).										
	SiO_2	Al_2O_3	Na_2O	Fe_2O_3	K_2O	CaO	MgO	SO_3	TiO_2	LOI
Fly ash	47.82	14.87	0.24	11.90	0.91	16.03	3.16	1.31	0.72	1.33
OPC, M350	20.73	5.85	0.21	2.79	0.39	60.99	2.21	2.47	–	2.93

For microstructural observation, small broken pieces from the mechanical testing were selected. Samples for scanning electron microscopy (SEM) observation were gold coated and observed using a JEOL JSM-6390 A SEM with an acceleration voltage of 30.0 kV. Transmission electron microscope (TEM) was carried out with a Technai electron microscope (Philips) on the powdered specimens.

Chemical composition of the used raw materials is shown in Table 3. For the OPC was used the cement produced by MAK LLC. Mongolia for concrete M350 type.

The chemical composition of the fly ash indicates relatively high content of sulfate and calcium oxide. According to ASTM C618 standard [21] the present fly ash belongs to class C high calcium fly ash. The fly ash should have both pozzolanic and self-cementing properties.

3. Results and discussion

3.1. Mechanical behaviour

Cylindrical specimens were kept immersed in water and after the required time were removed from the water and their compressive strengths measured. The core drilled samples were taken from the panels after exposure to normal outside Ulaanbaatar conditions. The official daytime temperature data for November 2017 to February 2018, the coldest months in Ulaanbaatar, averaged from −15 to −26 °C [22]. Obviously, the concrete panels cured in atmospheric condition panels had been subject to various atmospheric conditions including air temperature fluctuation, rain and snow. Therefore, in order to determine true compressive strength at the early stages cylindrical samples cured in water was used.

The compressive strength development of the water-aged samples is shown in Fig. 1.

It is observed that the compressive strength data of the cylindrical specimens aged in water show similar gradual increase with increasing aging time.

The concrete sample containing activated fly ash shows significant larger value at 28, 60, 120 days compared to the non-fly ash containing concretes. In other words, addition of mechanically activated fly ash enhances compressive strength of the concrete substantially. However, raw fly ash added specimens have a lower compressive strength than non-fly ash added specimens. Because of the pozzolanic reaction the compressive strength of the raw fly ash added concrete gets closer to the non-fly ash added specimen. From Fig. 1 the 3-day compressive strength of the non-fly ash added cylindrical specimens was 25.7 MPa, while it reduced to 19.7 MPa in the 20% fly ash substituted specimen and milled fly ash substituted specimen showed 23.1 MPa. However, the 28-day compressive strength of the non-fly ash added concrete specimen increased to 61.1 MPa, the raw fly ash added

specimen was 54.4 MPa and mechanically activated fly ash added specimen was 64.7 MPa. One can be seen that after 3 days the compressive strength of the material containing milled fly ash is approximately similar to the non-fly ash added concrete. The compressive strength of the material containing mechanically milled fly ash is higher after 28 days. Therefore, it is suggested that during the initial curing time, in the milled fly ash containing specimen, the accelerated pozzolanic reaction due to the reduction of the particle size and amorphization of the fly ash is responsible for the high compressive strength.

Compressive strength of the OPC concrete depends on gel structure and porosity. Gel structure is generally formed by hydration reaction of the OPC. Core drilled specimens taken from the ambient temperature cured outdoor concrete plates showed weaker compressive strength than the in water aged specimens. The compressive strength of the core drilled specimens was 26.6, 25.4 and 35.9 MPa for the non-fly ash added, raw fly ash added and activated fly ash added samples, respectively. Weak compressive strength of the ambient temperature cured concretes may be caused by slower hydration reaction rate and also possibly by stress initiated by core drilling process.

In the fly ash containing specimen were expected two types of reaction effects:

- The "ball bearing effect" where the spherical morphology of the fly ash results in a high packaging density in the concrete and good mechanical properties.
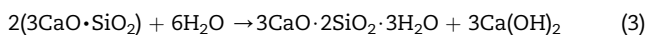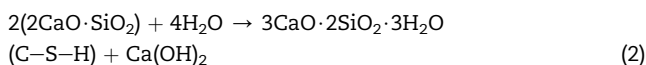- Accelerated pozzolanic reaction of the mechanically-activated fly ash.
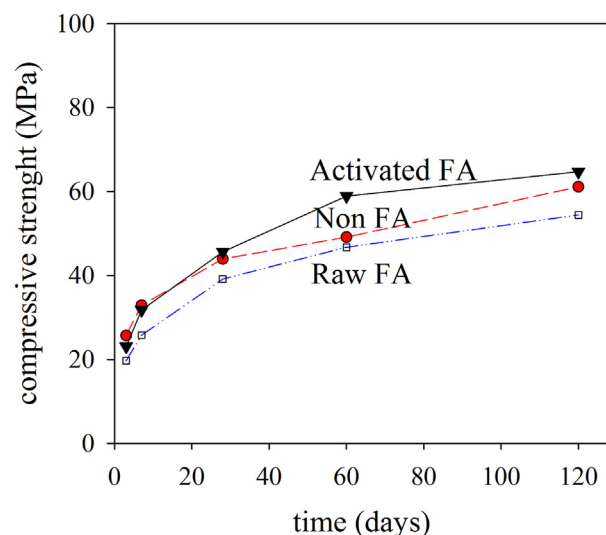
Fig. 1 – Change of compressive strength of concrete specimens with time.
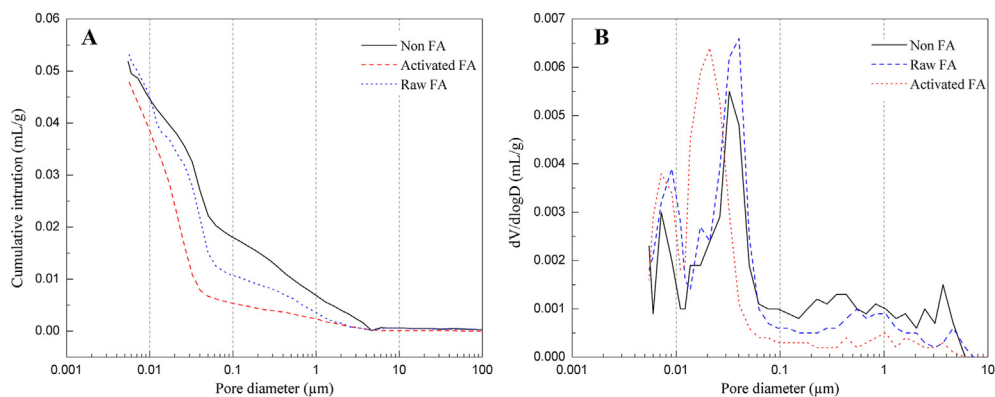
Fig. 2 — MIP measurements results for the concrete specimens, Cumulative intrusion (A) and Log differential intrusion.

Mechanical activation generally destroys spherical morphology of the fly ashes and reduces the "ball bearing effect". On the other hand, amorphization of the fly ash should result in a favorable pozzolanic reaction. Hydration of the belite and alite phases of OPC releases both the C—S—H phase and also calcium hydroxide, Ca(OH)$_2$ according to:

$$2(2CaO \cdot SiO_2) + 4H_2O \rightarrow 3CaO \cdot 2SiO_2 \cdot 3H_2O$$
$$(C-S-H) + Ca(OH)_2 \qquad (2)$$

$$2(3CaO \cdot SiO_2) + 6H_2O \rightarrow 3CaO \cdot 2SiO_2 \cdot 3H_2O + 3Ca(OH)_2 \qquad (3)$$

Mechanically treated fly ash should show a more favorable pozzolanic reaction than untreated fly ash expressed by Eq. (1).

Pozzolanic reactions with fly ashes occurs over a longer time span and can be started after more than 28 days when using low calcium fly ash [23].

3.2. Microstructural analysis

Fig. 2 shows mercury intrusion porosimetry (MIP) measurements results for the concrete specimens, Cumulative intrusion (A) and Log differential intrusion. Activated fly ash containing concrete shows fewer pores with larger diameter as shown by the cumulative intrusion and integral pore distribution curves (Fig. 2).

Another factor, that is usually associated with the compressive strength of the concrete is its microstructure development. The microstructure of the concrete can be evaluated by porosity measurements. Table 4 shows porous properties of the concrete specimens.

There is a pore nomenclature by IUPAC which shows presence of micropores less than 2 nm, mesopores in size of between 2 and 50 nm and macropores over 50 nm [24]. But it differs to those described by Kumar and Bhattacharjee [25] as

gel pores with size of 0.5—10 nm, capillary mesopores with average radius of 5—5000 nm and Mehta and Monteiro [26] who suggested that interparticle space within C—S—H phase will have sizes of 1—3 nm and capillary voids from 10 to 50 nm. It should be noted that there is no standard pore nomenclature for cement based materials.

Kumar and Bhattacharjee [25] studied the relation between porosity and compressive strength of concrete. It was suggested that the main effect on compressive strength shows when the capillary mesopores pores and macropores have a radius of over 5—5000 nm. Chen et al. [27] measured strength of the cement mortar and observed its decrease with increasing porosity.

Previous research mostly agrees and indicated that the mechanical properties of the concrete at the various stages of curing and application depend on its porous structure and their changes [28].

The present research indicated that there is little difference in pore sizes between the raw fly ash added and non fly ash added concretes. They have the main pore size distribution at 0.04, 0.007 and 0.009 μm sizes. Moreover, the number of pores increases with raw fly ash addition. However, activated fly ash added concrete showed a decrease in the pore size distribution to 0.02 μm and increase in pores with size of 0.007 μm. These pores are within the range of gel pores or C—S—H phase related pores.

Zhao et al. [29] suggested that the compressive strength of the cement mortar depends on porosity, mean diameter, and hydration degree. Liu et all [30]. observed a decrease in larger pores with addition of up to 30% of fly ash as cement substitute and the pores becoming less interconnected. These were attributed by filling of the pores by fine fly ash particles and formation of a C—S—H type phase by secondary hydration. In other words, the pore size reduction behaviour can be explained by filling the pores with the finer fly ash particles

Table 4 — Porous properties of the concrete specimens.				
Specimens	Properties			
	Porosity, %	Average pore diameter, nm	Total pore area, m^2/g	Intrusion volume, mL/g
Non-fly ash added concrete	9.40	25.3	8.19	0.0518
Raw fly ash added concrete	9.55	18.3	11.34	0.0519
Activated fly ash added concrete	9.04	16.1	12.06	0.0484
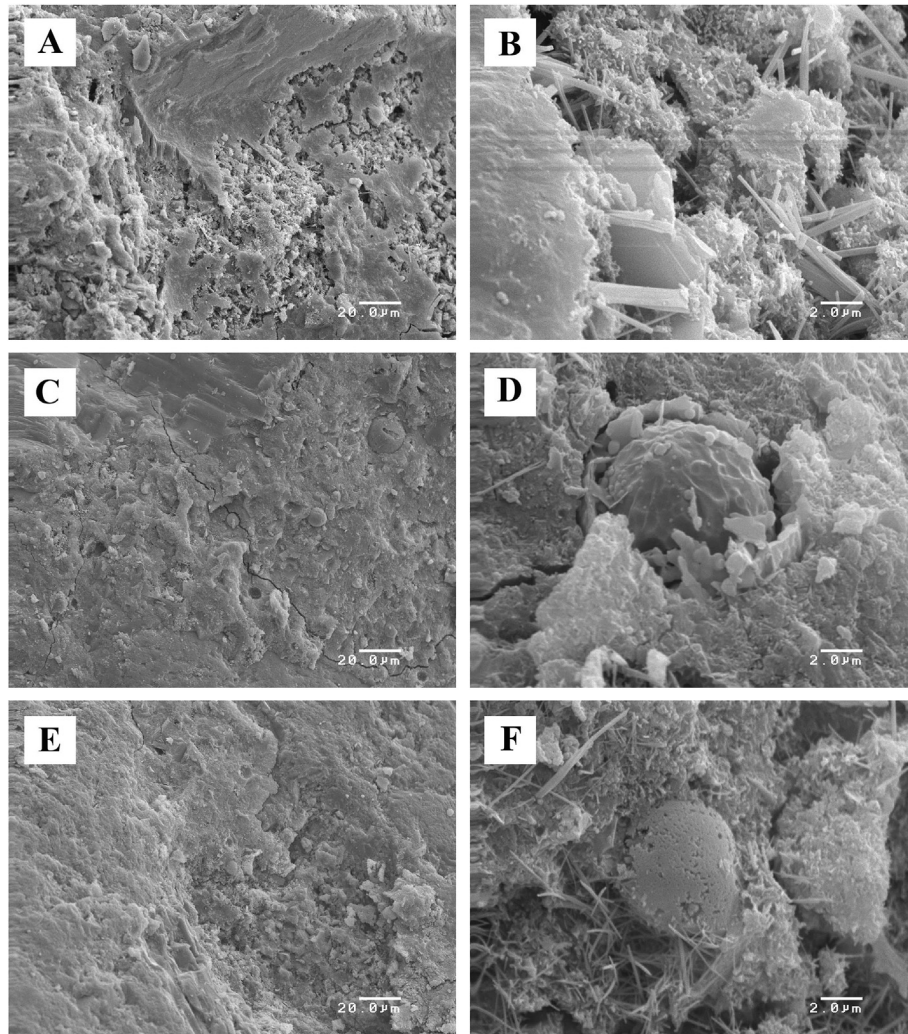
Fig. 3 – **SEM micrographs of the non-fly ash (A, B), raw fly ash (C, D) and activated fly ash (E, F) added concrete specimens.**

and generation of the C−S−H type phases within the pores by active pozzolanic reaction between the fly ash and portlandite [28].

Dissolution of the glassy fly ash particles by pozzolanic reaction was considered to be the main reason for the secondary hydration with the appearance of a low connectivity pore system. Dissolution of the glassy phase in the fly ash occurs more in the milled fly ash containing system, thus there is a more extensive pozzolanic reaction. It is possibly that the finer particle size and reactive surfaces of the milled fly ash is the main reason for the accelerated pozzolanic reaction.

The porosity measurements of the present research correlates well with the compressive strength results and is consistent with the research of Liu et al. [30]. A decrease in the 0.04 to 0.02 μm pores and an increase in the 0.007 μm pores resulted in denser microstructure combined by C−S−H type gel was the main reason of improved compressive strength of the activated fly ash added concrete. Approximate amorphous content of the specimens measured by XRD (not shown) for non-fly ash added concrete was 23%, raw fly ash added concrete 15% and activated fly ash added specimen was 25%.

Amorphous content could also be correlated with the C−S−H type gel but not with any C−S−H type crystalline phases [26]. In other words, activated fly ash added to concrete contains more gel structure.

Feng et al. [19] also observed that for ground fly ash added mortar the number of <20 nm pores increases while pores >20 nm decreases resulting in a denser microstructure. Since, the secondary pozzolanic reaction occurs continuously during the application, the improvement of the mechanical properties can be occurred continuously at late age of curing.

The microstructure of the samples as evaluated by SEM images supports the porosity measurements (Fig. 3).

Non-fly ash added or activated fly ash added concretes contain needle-like phases which could be either ettringite ($Ca_6Al_2(SO_4)_3(OH)_{12} \cdot 26H_2O$) (although this was not identified during XRD) or C−S−H ($CaO-SiO_2-H_2O$) phase. In the SEM of non-milled fly ash added specimen outer surface of fly ash sphere was leached out and inner surface seems to have been less affected. It may be that the fly ash spheres their surfaces affected by portlandite, one of the reaction products of the cement type reaction beside the C−S−H phase. In the milled fly ash containing concrete the fly ash surface was affected
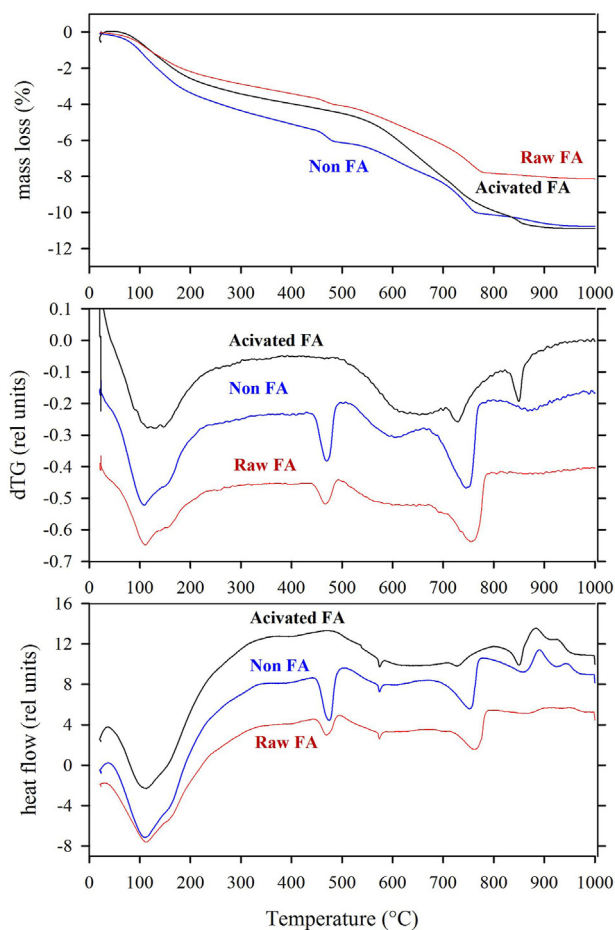
Fig. 4 − TG-DTG-DTA graph of the concrete samples.

with formation of the porous microstructure. Likely the surface had silica leached out forming the C−S−H phase. Moreover, the fly ash surface was surrounded by the gel type structure with some needle, possible by the presence of either ettringite or C−S−H phase.

3.3. Thermal behaviour

Fig. 4 shows TG, differential thermogravimetric (dTG) and DTA measurements of the concrete samples.

The total mass loss (TG) of the concrete containing activated fly ash is with about 10.5% in close agreement with the mass loss also obtained for concrete without fly ash. However, a clearly different rate of mass loss with temperature can be observed. The concrete containing raw fly ash showed a total mass loss of about 8.1%. The portions observed could be somehow intermediate between the concrete containing activated fly ash and that without fly ash addition.

Although the mass loss occurs gradually over the whole temperature range investigated, three main temperature ranges may be distinct.

I. **50−200°C.** Here mass loss is predominantly due to dehydration of water molecules through open pores. The dTG curves, i.e. the differential mass loss, show two

separate mass losses centred around 100 and 150 °C. These two peaks correspond to endothermic processes identified at the same temperature in the DTA curves. The first endothermic peak centred around 100 °C belongs to dehydration of the free water from the cement paste. The second endothermic peak is thought to be related with dehydration of C−S−H or/and calcium aluminium silicate hydrate (CASH) phases. The total loss at 200 °C is 4%, 3% and 2.5% for non-fly ash (non FA), activated fly ash (activated FA) and raw fly ash (raw FA) containing concretes, respectively.

II. **200−500°C.** The total loss in this temperature range is about 2%, 1% and 1% for non FA, activated FA and raw FA containing concretes, respectively. A pronounced dehydration of $Ca(OH)_2$ for concrete without FA of about 1% as identified by the peak with a maximum at 480 °C in the dTG and DTA curves [31]. It is observed that the $Ca(OH)_2$ content is lower in the raw FA added concrete, i. e about 0.5%, and is absent in the activated FA containing concrete.

III. **500−900°C.** This temperature range is characterized by the largest loss of about 6.5% for activated FA containing concrete. For non FA concrete and raw FA containing concrete the total loss was about 4.5%.

In all cases there are characteristic endothermic peaks superimposed on a broad endothermic curve which extends across the whole temperature range. All the endothermic effects correspond to peaks in the dTG curves without the effect at 573 °C which is only present in the DTA curves. This peak is related to the low quartz to high quartz phase transition. The intensity of this peak indicates similar contents in the three concrete samples. The remaining three endothermic effects are related to decarbonation indicating different stabilities of the carbonate which could be related to different growing conditions and structural details.

Firstly, the concrete containing activated FA shows a most pronounced broad endothermic effect with a maximum in the range 600−700 °C, similar to the broad effect also observed in the dTG curve. A similar peak is also observed in the non FA concrete at a lower temperature. Secondly, the endothermic peak with maximum at about 760 °C is strongest for the non FA concrete, smaller for the raw FA concrete, and smallest for the activated FA concrete. This peak corresponds to mass losses of 2% and 1% for non FA and raw FA concrete, respectively. Thirdly a rather sharp and strong endothermic peak is observed with a maximum at about 850 °C for activated FA concrete, which corresponds to about 0.5% of mass loss. A corresponding peak in non FA concrete appears rather broad and nearly negligible in raw FA concrete. This peak appears to be rather characteristic for the decarbonation of well grown calcite. The broader peak with maximum in the range 600−700 °C and the sharper peak at about 760 °C could also be observed in the thermal behaviour of limestone. It may be noted that two exothermic peaks with maximum at about 880 and 950 °C were observed for activated FA concrete. Similar peaks appear to be shifted towards higher temperatures for non FA concrete, and become nearly invisible for raw FA concrete. These exothermic effects could be related to crystallization of C_2S phases.
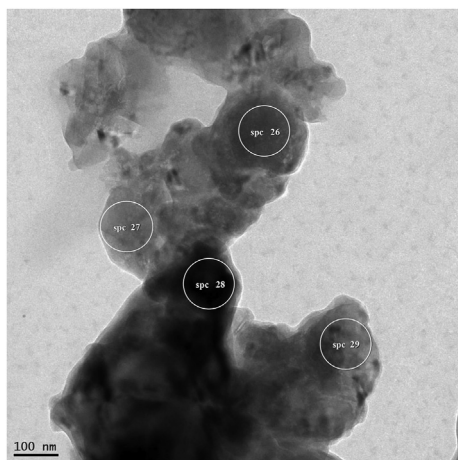
Fig. 5 — TEM micrograph of the milled fly ash added concrete.

Activated fly ash containing concrete shows no effect related to decomposition of portlandite from the hydration reaction of the cement. Obviously, it was consumed by pozzolanic reaction between the activated fly ash and portlandite according to reaction (1). The thermal and microstructural characterization of the concretes very well indicates the pozzolanic reaction products variability within the concrete specimens and in agreement each other (Figs. 2—4).

3.4. The pozzolanic reaction between the fly ash and cement components in concrete

The higher degree of reaction of activated FA concrete may also be related to a higher degree of carbonation. Thus, the decarbonation reaction is strongest in the activated FA concrete. The formed binder phase composition may also be different in the activated fly ash concrete compared to the non FA concrete. For non FA concrete it is known that the loss of strength occurs mainly between 200 and 500 °C related to the destruction of C—S—H phases due to dehydration. In this sense this effect

appears weaker in activated FA concrete. Here we assume a more effective formation of silica gel in a network and thus a destruction of C—S—H phases and a higher degree of carbonation. Such a reaction may not be realized by raw fly ash addition. The binder itself always compromise C—S—H type phase and gel type networks to more or less extend. Thus, we argue that the activated fly ash shows a formation of more gel type binder compared to non fly ash concrete.

Morphology difference of C—S—H phases formed in pure OPC and in the cement and supplementary cementitious materials blend was described and noted appearance of "foil" like structure in the supplementary cementitious materials blend [32].

Fig. 5 shows TEM micrograph of the milled fly ash added concrete.

The morphology of the circled regions shows similar to foil like C-S-H phase which was shown previously [32]. Table 5 shows chemical composition at selected regions of the milled fly ash added concrete. X-ray analyses of the circled regions (Table 5) show the presence of calcium, silica and aluminium atoms which indicates C—S—H and CASH phases are present in these regions. This suggests that concrete cured under ambient conditions has a lower compressive strength than the same concrete cured under standard condition, i.e. underwater. The general tendency of compressive strength change follows the same trend with standard cured concretes.

This secondary ettringite reaction may occur in concretes cured at normal temperatures.

All regions show the presence of the aluminium, this was almost certainly released from the fly ash during the pozzolanic reaction. Wang et al. [33] considered this to be due to the participation of the released Al and Si tetrahedra in pozzolanic reaction due to an increase in the alumino-silicate chains in C—S—H structure at middle or late age as it was observed by MIP and compressive strength measurements. The present research agrees with the conclusions drawn by Wang et al. [33].
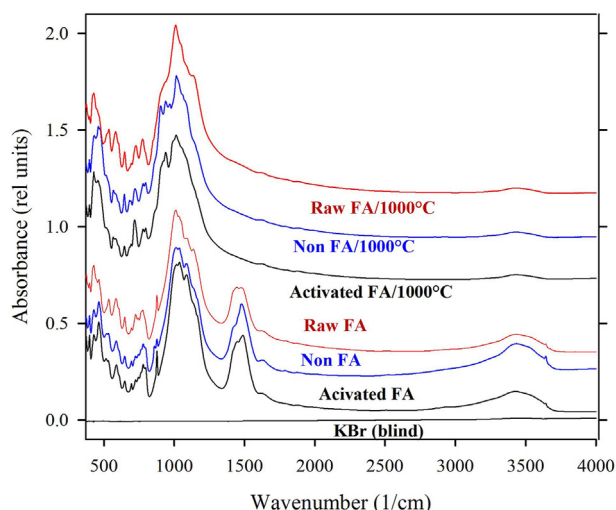
Fig. 6 shows IR absorption spectra of the concrete samples and spectra taken on the powders after DTA-TG measurements.

The IR spectra of the non fly ash added concrete resembles the activated fly ash added concrete. This could be an indication of the presence of a more homogeneous structure in

Table 5 — Chemical composition of the selected regions.

Area	Element	Weight, %	Atomic, %	Area	Element	Weight, %	Atomic, %
26	Mg	0.8	1.1	28	Na	3.8	5.2
	Al	8.3	11		Mg	1.3	1.6
	Si	27.2	34.8		Al	14.3	16.6
	S	1.2	1.3		Si	40.5	45.4
	K	0.3	0.3		S	1.5	1.5
	Ca	43.7	39.1		K	1.5	1.2
	Ti	4.1	3.1		Ca	34	26.7
	Mn	0.5	0.4		Fe	3.2	1.8
	Fe	13.9	8.9	29	Na	0.7	1
27	Al	6.9	8.5		Mg	2.7	3.8
	Si	41.7	49.7		Al	8.8	11.2
	K	0.9	0.8		Si	26.3	32
	Ca	45.6	38		S	1.7	1.8
	Fe	4.9	2.9		K	1.4	1.3
					Ca	54.8	46.8
					Fe	3.6	2.2

Fig. 6 – IR absorption spectra of the concrete samples before and after DTA-TG measurements.

both milled fly ash and non fly ash containing concretes compared to that of raw fly ash containing concrete. All 3 concrete specimens showed a peak at 3642 cm^{-1} due to portlandite. However, from Fig. 4 activated fly ash containing concrete did not show portlandite decomposition by heating. Probably the content of the portlandite in the concrete wasn't high enough to detect by DTA-TG. Similar absorption bands for all 3 samples belong to water at 1430 and carbonate at 1640 cm^{-1}. After DTA-TG measurements the absorption peak for water disappeared, however, carbonate peak is still being observable due to atmospheric carbonation.

Experimental results indicate the presence of different behaviour by adding mechanically milled fly ash to the concrete cured at atmospheric condition:

- Fly ash particle size reduction by milling is more effective than particle size reduction by sieving or separation.
- Milled fly ash shows a more extensive pozzolanic reaction than non-milled fly ash.
- With fly ash milling occurs amorphization that shows positive influence on the pozzolanic reaction.
- Milling of fly ash destroys its spherical morphology thereby reducing the ball bearing effect leading to an increasing water demand for concrete preparation and is consequently expected to reduce the pozzolanic reaction. In contrast, mechanical amorphization and ready interaction with portlandite overweighs the higher water demand of the less spherical morphology.

Therefore, the beneficial occurrence of the pozzolanic reaction is thought to be the main reason for the improved compressive strength.

4.   Conclusions

The substitution of 20% OPC with milled fly ash increases the compressive strength of ambient temperature cured concrete

by 25% after 1 year curing. Reduction of the particle size of the fly ash with the appearance of a fresh glassy surface is the main reason for a beneficial pozzolanic reaction in the mechanically activated fly ash containing concrete. The pozzolanic reaction in concrete substituted with raw fly ash appears somewhat slower. Mechanically activated fly ash results in higher compressive strength concrete after 28 days in specimens cured under standard conditions. Mechanically activation of fly ash allows the formation of a gel-type phase by secondary hydration and carbonation resulting in a reduction of the pore sizes due to the coarser pores filling with gel.

Although, the pozzolanic reaction rate in the concrete cured at atmospheric condition is not fast, addition of mechanically activated fly ash allows the formation of a denser microstructure after longer timespan.

DTA-TG showed that milled fly ash added concrete has a beneficial pozzolanic reaction rate as indicated by the formation of less portlandite than in the non-fly ash and raw fly ash added OPC concretes. The carbonation reaction rate also decreases from non-fly ash added to raw fly ash added and was lowest in the mechanically activated fly ash added concretes.

Declaration of Competing Interest

The authors declare that they have no known competing financial interests or personal relationships that could have appeared to influence the work reported in this paper.

Acknowledgements

R E F E R E N C E S

[1] Blezard RG. The history of calcareous cements. In: Hewlett PC, editor. Lea's chemistry of cement and concrete. ed. Oxford: Elsevier; 1998. p. 1–23 [Chapter 1].

[2] Phair JW. Green chemistry for sustainable cement production and use. Green Chem 2006;8:763–80. https://doi.org/10.1039/B603997A.

[3] ACI 232.2r-96. Use of fly ash in concrete. American Concrete Institute; 1996. http://civilwares.free.fr/ACI/MCP04/2322r_96.pdf/ [accessed December 2021].

[4] Labrincha J, Puertas JF, Schroeyers W, Kovler K, Pontikes Y, Nuccetelli C, et al. From NORM by-products to building materials. In: Schroeyers W, editor. In: schroeyers, W. Naturally occurring radioactive materials in construction, integrating radiation protection in reuse. Kidlington. Woodhead publishing; 2017. p. 183–252 [Chapter 7].

[5] Thomas M. Optimizing the use of fly ash in concrete, Portland cement association. https://www.cement.org/docs/default-source/fc_concrete_technology/is548-optimizing-the-use-of-fly-ash-concrete.pdf; [accessed January 2022].

[6] Temuujin J, Surenjav E, Ruescher CH, Vahlbruch J. Review Processing and uses of fly ash addressing radioactivity

(critical review). Chemosphere 2019;216:866–82. https://doi.org/10.1016/j.chemosphere.2018.10.112.

[7] Temuujin J, Williams R, Van Riessen A. Effect of mechanical activation of fly ash on the properties of geopolymer cured at ambient temperature. J Mat Process Tech 2009;209:5276–80. https://doi.org/10.1016/j.jmatprotec.2009.03.016.

[8] Thomas MDA, Shehata MH, Shashiprakash SG. Cement, concrete and aggregates, the use of fly ash in concrete: classification by composition. Cem Concr Aggregates 1999;21:105–10. https://doi.org/10.1520/CCA10423J.

[9] Xu G, Shi X. Characteristics and applications of fly ash as a sustainable construction material: a state-of-the-art review. Res Conserv Recycl 2018;136:95–109. https://doi.org/10.1016/j.resconrec.2018.04.010.

[10] Juenger MCG, Siddique R. Recent advances in understanding the role of supplementary cementitious materials in concrete. Cement Concr Res 2015;78:71–80. https://doi.org/10.1016/j.cemconres.2015.03.018.

[11] Scrivener KL, Juilland P, Monteiro PJM. Advances in understanding hydration of Portland cement. Cement Concr Res 2015;78:38–56. https://doi.org/10.1016/j.cemconres.2015.05.025.

[12] Li Z, Xu G, Shi X. Reactivity of coal fly ash used in cementitious binder systems: a state-of-the-art overview. Fuel 2021;301:121031. https://doi.org/10.1016/j.fuel.2021.121031.

[13] Li Y, Wu B, Wang R. Critical review and gap analysis on the use of high-volume fly ash as a substitute constituent in concrete. Const Build Mat 2022;341:127889. https://doi.org/10.1016/j.conbuildmat.2022.127889.

[14] Kumar R, Kumar S, Melhotra SP. Review: towards sustainable solutions for fly ash through mechanical activation. Res Conserv Recycl 2007;52:157–79. https://doi.org/10.1016/j.resconrec.2007.06.007.

[15] Kumar S, Kumar R. Mechanical activation of fly ash: effect on reaction, structure and properties of resulting geopolymer. Ceram Int 2011;37:533–41. https://doi.org/10.1016/j.ceramint.2010.09.038.

[16] Bicer A. Effect of fly ash particle size on thermal and mechanical properties of fly ash-cement composites. Therm Sci Eng Prog 2018;8:78–82. https://doi.org/10.1016/j.tsep.2018.07.014.

[17] Han X, Yang J, Feng J, Zhou C, Wang X. Research on hydration mechanism of ultrafine fly ash and cement composite. Constr and Build Mat 2019;227:116697. https://doi.org/10.1016/j.conbuildmat.2019.116697.

[18] Chu YS, Davaabal B, Kim DS, Seo SK, Ruescher C, Temuujin J. Reactivity of fly ashes milled in different milling devices. Rev Adv Mater Sci 2019;58:179–88. https://doi.org/10.1515/rams-2019-0028.

[19] Feng J, Sun J, Yan P. The influence of ground fly ash on cement hydration and mechanical property of mortar. Adv Civ Eng 2018;2018:4023178. https://doi.org/10.1155/2018/4023178.

[20] Blanco F, Garcia MP, Ayala J, Mayoral G, Garcia MA. The effect of mechanically and chemically activated fly ashes on mortar properties. Fuel 2006;85:2018–26. https://doi.org/10.1016/j.fuel.2006.03.031.

[21] ASTM C618-19. Standard specification for coal fly ash and raw or calcined natural pozzolan for use in concrete, https://www.astm.org/c0618-19.html; 2019 [last accessed July 25 2022].

[22] Home page - Time and Date AS. [last cited 2022 June 15]. Available from: https://www.timeanddate.com/weather/mongolia/ulaanbaatar/historic?month=1&year=2018.

[23] Hemalatha T, Ramaswamy A. A review on fly ash characteristics e towards promoting high volume utilization in developing sustainable concrete. J Clean Prod 2017;147:546–59. https://doi.org/10.1016/j.jclepro.2017.01.114.

[24] Sing KSW, Everett DH, Haul RAW, Moscou L, Pierotti RA, Rouquerol J, et al. Reporting physisorption data for gas/solid systems with special reference to the determination of surface area and porosity. Pure Appl Chem 1985;57:603–19. https://doi.org/10.1515/iupac.57.0007.

[25] Kumar R, Bhattacharjee B. Porosity, pore size distribution and in situ strength of concrete. Cem Concr Res 2003;33:155–64. https://doi.org/10.1016/S0008-8846(02)00942-0.

[26] Mehta PK, Monteiro PJ M. Concrete: microstructure, properties, and materials. ed. New York: McGraw-Hill; 2006.

[27] Chen X, Wu S, Zhou J. Influence of porosity on compressive and tensile strength of cement mortar. Constr Build Mat 2013;40:869–74. https://doi.org/10.1016/j.conbuildmat.2012.11.072.

[28] Wang L, Jin M, Guo F, Wang Y, Tang S. Pore structural and fractal analysis of the influence of fly ash and silica fume on the mechanical property and abrasion resistance of concrete. Fractals 2021;29(2):2140003. https://doi/10.1142/S0218348X2140003X.

[29] Zhao H, Xiao Q, Huang D, Zhang S. Influence of pore structure on compressive strength of cement mortar. Sci World J 2014;2014:247058. https://doi.org/10.1155/2014/247058.

[30] Liu J, Tang K, Qiu Q, Pan D, Lei Z, Xing F. Experimental investigation on pore structure characterization of concrete exposed to water and chlorides. Mat 2014;7(9):6646–59. https://doi.org/10.3390/ma7096646.

[31] Sun J, Shen X, Tan G, Tanner JE. Modification effects of nano-SiO_2 on early compressive strength and hydration characteristics of high-volume fly ash concrete. J Mater Civ Eng 2019;31(6):04019057. https://doi.org/0.1061/(ASCE)MT.1943-5533.0002665.

[32] Scrivener KL, Nonat A. Hydration of cementitious materials, present and future. Cem Concr Res 2011;41:651–65. https://doi.org/10.1016/j.cemconres.2011.03.026.

[33] Wang L, Guo F, Lin Y, Yang H, Tang SW. Comparison between the effects of phosphorous slag and fly ash on the C-S-H structure, long-term hydration heat and volume deformation of cement-based materials, vol. 250. Constr Build Mat.; 2020. p. 118807. https://doi.org/10.1016/j.conbuildmat.2020.118807.